P H Y S I C A L   R E V I E W   L E T T E R S

J/ψ Suppression in *p-A* Collisions from Parton Energy Loss in Cold QCD Matter

François Arleo[1,2] and Stéphane Peigné[3]

[1]*Laboratoire d'Annecy-le-Vieux de Physique Théorique (LAPTh), UMR5108, Université de Savoie and CNRS,
BP 110, 74941 Annecy-le-Vieux cedex, France*
[2]*PH-TH Department, CERN, 1211 Geneva 23, Switzerland*
[3]*SUBATECH, UMR 6457, Université de Nantes, IN2P3/CNRS 4 rue Alfred Kastler, 44307 Nantes cedex 3, France*

The effects of energy loss in cold nuclear matter on *J/ψ* suppression in *p-A* collisions are studied. A simple model based on first principles and depending on a single free parameter is able to reproduce *J/ψ* suppression data at large x_F and at various center-of-mass energies. These results strongly support energy loss as a dominant effect in quarkonium suppression. They also give some hint on its hadroproduction mechanism suggesting color neutralization to happen on long time scales. Predictions for *J/ψ* and Υ suppression in *p*-Pb collisions at the LHC are made.

The spectacular results on jet production in Pb–Pb collisions at the LHC (see, e.g., Refs. [1,2]) find a natural explanation in terms of parton energy loss in quark-gluon plasma. Despite the wealth of data accumulated so far at RHIC and LHC, the in-depth understanding of energy loss processes remains far from complete (see Ref. [3] for a discussion). Recently, new scaling properties have been identified for the induced gluon radiation spectrum, $dI/d\omega$, of hard processes where a color charge undergoes small angle scattering through a static medium (nuclear matter or quark-gluon plasma) [4].

The goal of this Letter is to explore the phenomenological consequences of these results on *J/ψ* as well as Υ suppression,

$$R_{pA}(x_F) = \frac{d\sigma_{pA}^{J/\psi}}{dx_F}(x_F) \bigg/ \frac{Ad\sigma_{pp}^{J/\psi}}{dx_F}(x_F), \quad (1)$$

in *p-A* and *π-A* collisions (we keep in the following the notations "*J/ψ*" and "*p-A*" for clarity). This observable allows for probing energy loss in nuclear matter, which is a well-controlled medium as opposed to an expanding quark-gluon plasma in which the dynamics are more complex. Moreover, understanding quarkonium suppression in *p-A* collisions is a prerequisite in order to interpret quantitatively the measurements performed in heavy-ion collisions at the LHC [5–7]. It is striking that there is no consensus yet on the origin of the significant *J/ψ* suppression reported at large rapidity in *p-A* collisions, from SPS to RHIC [8–10], despite many theoretical attempts (see Ref. [11] for a review).

As is well known, quarkonium hadroproduction in elementary *p-p* collisions is not fully understood. In order to study quarkonium nuclear suppression in the most model-independent way, the *p-p* quarkonium production cross section will be taken from experiment. We will only assume that the heavy-quark $Q\bar{Q}$ pair is produced in a compact color octet state, within the hard process time

scale t_h, and remains color octet for a time much longer than t_h. In quarkonium production models where color neutralization is a soft, nonperturbative process, this assumption holds at any x_F. In the color singlet model, we expect this assumption to be founded at large enough x_F, where the gluon emission required for color neutralization is constrained to be semihard (or even softish) by energy conservation. With this assumption, at sufficiently large quarkonium energy E in the target rest frame, quarkonium hadroproduction looks like small angle scattering of a color charge [12]. The associated soft gluon radiation spectrum is thus similar to the (non-Abelian) Bethe-Heitler spectrum of an asymptotic charge and depends on the amount of transverse momentum kick $q_\perp$ to the charge. The typical $q_\perp$ is expected to be larger in *p-A* than in *p-p* collisions due to transverse momentum nuclear broadening $\Delta q_\perp^2$. As a result, the medium-induced radiation spectrum is similar to the Bethe-Heitler spectrum with $q_\perp^2$ replaced by $\Delta q_\perp^2$ (see Ref. [4]),

$$\omega \frac{dI}{d\omega} = \frac{N_c \alpha_s}{\pi} \left\{ \ln\left(1 + \frac{\Delta q_\perp^2 E^2}{M_\perp^2 \omega^2}\right) - \ln\left(1 + \frac{\Lambda^2 E^2}{M_\perp^2 \omega^2}\right) \right\}. \quad (2)$$

In the following, we shall take $\alpha_s = 0.5$, $\Lambda = \Lambda_{QCD} = 0.25$ GeV, $p_\perp = 1$ GeV in the transverse mass $M_\perp = \sqrt{M^2 + p_\perp^2}$, and $M = 3$ GeV ($M = 9$ GeV) for the mass of a compact $c\bar{c}$ ($b\bar{b}$) pair.

This leads to an average medium-induced radiative loss scaling as the quarkonium energy, $\Delta E \propto E$. In the limit $\Lambda^2 \ll \Delta q_\perp^2 \ll M_\perp^2$ we have

$$\Delta E \equiv \int_0^E d\omega \, \omega \frac{dI}{d\omega} \simeq N_c \alpha_s \frac{\sqrt{\Delta q_\perp^2}}{M_\perp} E. \quad (3)$$

The scaling $\Delta E \propto E$ was first postulated in Ref. [13] (also revisited in Ref. [14]) yet this assumption was not motivated and the parametric dependence on L and M arbitrary

[and different from Eq. (3)]. In Ref. [15], a bound on medium-induced energy loss was derived, $\Delta E \lesssim E^0$ but in a specific setup where the nuclear broadening of the final tagged particle was neglected.

The starting point of the model consists in expressing the J/ψ differential production cross section $d\sigma/dx_F$ in p-A collisions simply as that in p-p collisions, with a shift in x_F accounting for the energy loss ε incurred by the octet $c\bar{c}$ pair propagating through the nucleus,

$$\frac{1}{A}\frac{d\sigma_{pA}^{J/\psi}}{dx_F}(x_F) = \int_0^{\min(E_p-E,E)} d\varepsilon\, \mathcal{P}(\varepsilon)\frac{d\sigma_{pp}^{J/\psi}}{dx_F}[x_F + \delta x_F(\varepsilon)],$$
(4)

where x_F is defined as the longitudinal momentum fraction between the J/ψ and projectile proton in the c.m. frame of an elementary p-N collision (of energy $\sqrt{s}$). In the limit $\sqrt{s} \gg m_p$ (with m_p the proton mass), it reads

$$x_F = x_F(E) = \frac{E}{E_p} - \frac{E_p}{E}\frac{M_\perp^2}{s},$$
(5)

where E and $E_p \simeq s/(2m_p)$ are respectively the $c\bar{c}$ pair and projectile proton energies in the nucleus rest frame. We now describe the various ingredients in Eq. (4). (i) The differential p-p cross section is determined from a fit of p-p data and can be conveniently parametrized as

$$\frac{d\sigma_{pp}^{J/\psi}}{dx_F}(x_F) \propto (1 - x')^n/x'; \qquad x' \equiv \sqrt{x_F^2 + 4M_\perp^2/s}. \quad (6)$$

The exponent n is extracted from p-p data taken at the same c.m. energy (whenever possible) as the p-A measurements discussed in this Letter [the normalization parameter being irrelevant for our purpose, see Eq. (1)]; (ii) The shift $\delta x_F(\varepsilon)$ is defined by

$$x_F(E) + \delta x_F(\varepsilon) = x_F(E+\varepsilon) = \frac{E+\varepsilon}{E_p} - \frac{E_p}{E+\varepsilon}\frac{M_\perp^2}{s},$$
(7)

where E is obtained directly from Eq. (5). Note that at large $x_F \gg M_\perp/\sqrt{s}$, we have $E \simeq x_F E_p$ and $\delta x_F(\varepsilon) \simeq \varepsilon/E_p$; (iii) The average over ε in Eq. (4) is performed using the energy loss probability distribution, or quenching weight $\mathcal{P}(\varepsilon)$. As a simple and physically sound choice for a normalized distribution, we take [16]

$$\mathcal{P}(\varepsilon) = \frac{dI}{d\varepsilon}\exp\left\{-\int_\varepsilon^\infty d\omega \frac{dI}{d\omega}\right\}.$$
(8)

The amount of medium-induced gluon radiation, and hence the strength of J/ψ suppression in p-A collisions, is controlled by $\Delta q_\perp^2$ in Eq. (2). For a path length L travelled across the target (proton or nucleus), it reads

$$\Delta q_\perp^2(L) = \hat{q}_A L - \hat{q}_p L_p,$$
(9)

where the average path length is given by $L = \frac{3}{2}r_0 A^{1/3}$ ($r_0 = 1.12$ fm), assuming the hard process to occur uniformly in the nuclear volume. In Eq. (9), $\hat{q}_A$ (respectively $\hat{q}_p$) stands for the transport coefficient in the nucleus A (resp. in the proton). It is related to the gluon distribution $G(x)$ in a target nucleon as [17]

$$\hat{q}(x) = \frac{4\pi^2 \alpha_s(\hat{q}L)N_c}{N_c^2 - 1}\rho x G(x, \hat{q}L),$$
(10)

where ρ is the target nuclear density. Apart from the scaling violations in the running of α_s and in the evolution of the gluon density, both neglected since $\hat{q}L \lesssim 1$ GeV^2, the L dependence of $\hat{q}$ mainly enters via the typical x value at which $xG(x)$ should be evaluated. When the hard production time $t_h \ll L$, it is estimated to be $x \simeq (2m_p L)^{-1} \equiv x_0$ [17]. For large nuclei (e.g., W, Au, or Pb), this corresponds to $x_0 = \mathcal{O}(10^{-2})$. When $t_h \gg L$, the hard subprocess is coherent over the whole nucleus, and in this case, we expect $x \sim x_2$ [16], where x_2 is the target parton momentum fraction, $x_2 = (-x_F + x')/2$ when assuming a $2 \to 1$ subprocess kinematics. Using the power-law behavior $xG(x) \sim x^{-0.3}$ suggested by fits to small-x HERA data [18], $\hat{q}$ is thus given by

$$\hat{q}(x) = \hat{q}_0\left(\frac{10^{-2}}{x}\right)^{0.3}; \qquad x = \min(x_0, x_2). \quad (11)$$

In Eq. (11), the transport coefficient $\hat{q}_0 \equiv \hat{q}(x = 10^{-2})$ is the only free parameter of the model.

Besides energy loss effects, other mechanisms might affect J/ψ suppression in nuclei. At small energy E, when the J/ψ hadronization time $t_\psi = \gamma\tau_\psi \lesssim L$, J/ψ's are produced inside the nuclear medium and consequently might suffer inelastic interaction with the target nucleus or nuclear absorption. In the figures below, we indicate by an arrow the typical value of x_F below which this starts to happen, assuming $\tau_\psi \simeq 0.3$ fm. Another effect is the expected saturation of the nuclear gluon density at small x_2, leading to an additional J/ψ suppression in high-energy p-A collisions. The associated suppression is a scaling function of the saturation scale Q_s, which can be simply parametrized as [19]

$$\mathcal{S}_A^{\text{sat}}(x_2, L) \simeq \frac{a}{[b + Q_s^2(x_2, L)]^\alpha}.$$
(12)

In order to make reliable predictions at RHIC and LHC, where saturation effects might be important, the J/ψ nuclear production ratio will be determined assuming energy loss effects, $R_{pA}^{E.\text{loss}}$ from Eq. (4), with and without saturation effects,

$$\text{(i) } R_{pA} = R_{pA}^{E.\text{loss}}, \qquad \text{(ii) } R_{pA} = R_{pA}^{E.\text{loss}} \times \mathcal{S}_A^{\text{sat}}/\mathcal{S}_p^{\text{sat}}.$$

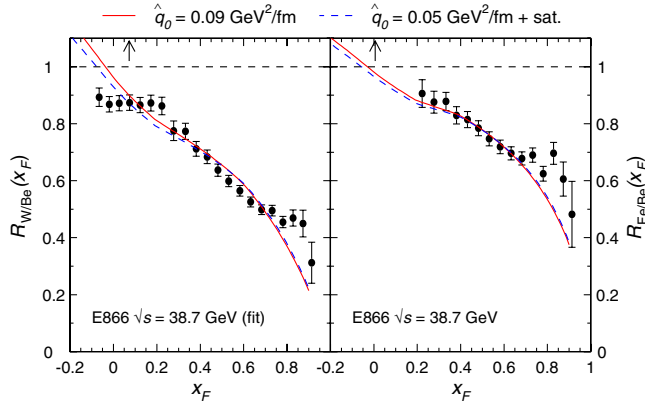The saturation scale appearing in Eq. (12) is determined consistently in our model through the relationship [20]

FIG. 1 (color online).   E866 J/ψ suppression data [9] in p-W (left) and p-Fe (right) collisions compared to the energy loss model.

$$Q_s^2(x, L) = \hat{q}(x)L, \qquad (13)$$

where $\hat{q}(x)$ is given by Eq. (11). The inclusion of saturation effects thus does not require any additional parameter.

The only parameter of the model, the transport coefficient $\hat{q}_0$, is determined by fitting the J/ψ suppression measured by E866 [9] in p-W over p-Be collisions at $\sqrt{s} = 38.7$ GeV in the [0.2–0.8] x_F range [21]. This choice is motivated by the fact that these data are the most precise measurements performed so far and cover a wide range in x_F. The fit gives $\hat{q}_0 = 0.09$ GeV^2/fm assuming energy loss effects only and $\hat{q}_0 = 0.05$ GeV^2/fm when saturation effects are also included. This x_F range corresponds to values of $x_2 = 0.01$–0.03 for which saturation effects are rather small, of the order of 5% on the W/Be ratio. The result of the fit in these two cases is shown in Fig. 1 (left panel); the agreement is excellent in the fit range, while a slight disagreement is observed below $x_F \lesssim 0.1$, where nuclear absorption is expected to play a role. The successful description of J/ψ suppression in iron, $R_{\text{Fe/Be}}$ (right panel), at the same energy fully supports the atomic mass dependence of the model. Note also that the values for the transport coefficient, $\hat{q}_0 = 0.05$–0.09 GeV^2/fm, would correspond to the saturation scale in a proton $Q_s^2(x = 10^{-2}) = 0.08$–0.15 GeV^2 using Eq. (13), which is consistent with (yet slightly smaller than) estimates based from fits to F_2 DIS data [22]. Note that the saturation scale in large nuclei and at smaller x considerably exceeds that in a proton, yielding $\hat{q}(x)L \sim 1$ GeV^2, where the use of perturbative techniques is commonly assumed to be legitimate.

Data taken at lower $\sqrt{s}$ or smaller x_F are also compared to the model. As can be seen in Fig. 2 the agreement is very good, both in shape and magnitude, over a very wide range in x_F. We also remark that, as expected, the model tends to slightly underestimate the suppression in the x_F domain where J/ψ's might hadronize inside the nucleus and suffer nuclear absorption; see in particular the comparison with NA60 [23] and HERA-B [24] data. It is also remarkable
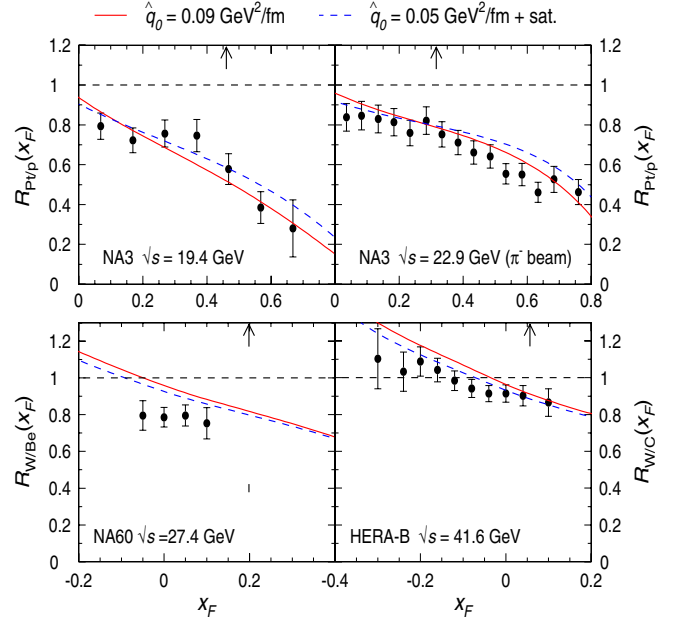

FIG. 2 (color online).   NA3 [8], NA60 [23], and HERA-B [24] J/ψ suppression data in p-A (π^--A) collisions compared to the energy loss model.

that the model is able to reproduce the different magnitude of suppression in p-A and π^--A collisions reported by NA3 [8] (Fig. 2, upper panels). This difference cannot be understood within nuclear absorption models (since factorization is usually assumed between the hard production process and final state interaction) nor can it be explained by nuclear parton distribution function (nPDF) effects, unless the nPDF to proton PDF ratios for valence quarks and for gluons, probed respectively in π^--A and p-A collisions, prove completely different. In our picture, the smaller J/ψ suppression in π^--A collisions naturally arises from the flatter differential cross section, $n_{\pi p} = 1.5$ vs $n_{pp} = 4.3$ [see Eq. (6)] at NA3 energies, a feature which can be explained from the slope of the PDF in a pion and in a proton, respectively. For completeness, the predictions including saturation are also shown as dashed lines in Fig. 2; as expected, saturation effects are tiny at these energies. The slight differences are essentially due to the smaller transport coefficient used ($\hat{q}_0 = 0.05$ GeV^2/fm) when saturation is included.

The predictions in d-Au collisions at RHIC, $\sqrt{s} = 200$ GeV, are shown in Fig. 3 in comparison with PHENIX data [10]. Energy loss effects are able to reproduce J/ψ suppression at positive rapidities. However, some disagreement is observed in the negative y bins for which nuclear absorption is expected to play a role; it has also been conjectured that a depletion of the gluon nPDF at large x_2 might explain the trend of the data at backward rapidities [25]. We also note that the disagreement is reduced when saturation effects are included. Finally, arguing about the possible slight disagreement observed
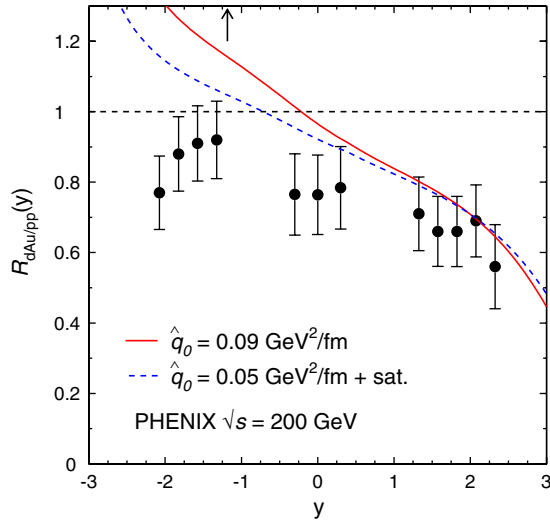
FIG. 3 (color online). PHENIX J/ψ suppression data [10] in
d-Au collisions compared to the energy loss model.

FIG. 4 (color online). J/ψ and Υ suppression expected in
p-Pb collisions at the LHC.

around midrapidity might be premature, given the present
experimental uncertainties.

Last, the rapidity dependence of J/ψ suppression in
p-Pb collisions at the LHC (taking $\sqrt{s} = 5$ TeV) is shown
in Fig. 4. Even though the inclusion of saturation effects is
expected to yield a stronger J/ψ suppression, it is some-
how compensated by the use of a smaller transport coeffi-
cient; as a consequence, predictions with (dashed line) and
without (solid) saturation are actually rather similar, except
in the negative y bins. As can be seen from the arrow in
Fig. 4, J/ψ hadronization should take place outside the
nuclear medium above $y \gtrsim -5$; nuclear absorption should
thus play little or no role at the LHC. At forward rapidities,
J/ψ suppression becomes rather large, e.g., $R_{pPb} \simeq$
0.7–0.8 at $y = 1$ down to $R_{pPb} \lesssim 0.5$ at $y \gtrsim 4$. Fig. 4
also shows the predicted Υ suppression as a dash-dotted
line. Because of the mass dependence of energy loss, $\Delta E \propto$
$M_\perp^{-1}$, it is expected to be smaller than that of J/ψ yet not
negligible, e.g., $R_{pPb}^\Upsilon \simeq 0.8$ at $y = 3$. These predictions can
be compared to the future measurements by the ALICE and
LHCb experiments during the p-Pb run scheduled in 2012.

In summary, an energy loss model (supplemented by
saturation effects) based on first principles has been pre-
sented. Once the transport coefficient is determined from a
subset of E866 data, it is able to reproduce nicely all
existing J/ψ measurements in p-A collisions. In particular
the dependence of J/ψ suppression on x_F, for various
atomic masses A and center-of-mass energies $\sqrt{s}$, is well
accounted by the model. These results strongly support
energy loss in cold nuclear matter to be the dominant effect
of J/ψ suppression, at least at large rapidities. It also
qualitatively explains why no suppression in inelastic
J/ψ electroproduction is observed [26], since Eq. (3)
does not apply to this case [4]. Finally, the agreement
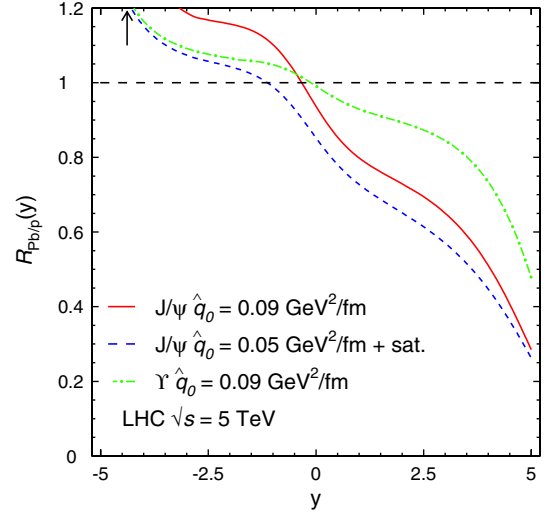between the data and our model predictions supports the

assumption of a long-lived color octet $Q\bar{Q}$ pair. As a
perspective, we plan to investigate energy loss effects on
J/ψ suppression in heavy-ion collisions as well as to
explore their consequences on other hard processes.

[1] G. Aad *et al.* (ATLAS), Phys. Rev. Lett. **105**, 252303
(2010).
[2] S. Chatrchyan *et al.*, Phys. Lett. B **712**, 176 (2012).
[3] N. Armesto *et al.*, arXiv:1106.1106.
[4] F. Arleo, S. Peigné, and T. Sami, Phys. Rev. D **83**, 114036
(2011).
[5] G. Aad *et al.*, Phys. Lett. B **697**, 294 (2011).
[6] S. Chatrchyan *et al.*, arXiv:1201.5069.
[7] B. Abelev *et al.*, arXiv:1202.1383.
[8] J. Badier *et al.*, Z. Phys. C **20**, 101 (1983).
[9] M. J. Leitch *et al.*, Phys. Rev. Lett. **84**, 3256 (2000).
[10] A. Adare *et al.*, Phys. Rev. Lett. **107**, 142301 (2011).
[11] A. D. Frawley, T. Ullrich, and R. Vogt, Phys. Rep. **462**,
125 (2008).
[12] We stress that the spectrum (2) and associated average loss
(3) are absent in Drell-Yan production, where no color
charge is produced at the production time t_h.
[13] S. Gavin and J. Milana, Phys. Rev. Lett. **68**, 1834
(1992).
[14] B. Z. Kopeliovich, J. Nemchik, I. K. Potashnikova, M. B.
Johnson, and I. Schmidt, Phys. Rev. C **72**, 054606 (2005).
[15] S. J. Brodsky and P. Hoyer, Phys. Lett. B **298**, 165 (1993).
[16] F. Arleo and S. Peigné (to be published).
[17] R. Baier, Y. L. Dokshitzer, A. H. Mueller, S. Peigné, and
D. Schiff, Nucl. Phys. **B484**, 265 (1997).

[18] K. J. Golec-Biernat and M. Wüsthoff, Phys. Rev. D **59,** 014017 (1998).

[19] H. Fujii, F. Gelis, and R. Venugopalan, Nucl. Phys. **A780,** 146 (2006).

[20] A. H. Mueller, Nucl. Phys. **B558,** 285 (1999); R. Baier, Nucl. Phys. **A715,** 209c (2003).

[21] Depending on the x_F range used for the fit, the resulting uncertainty on $\hat{q}_0$ is of the order of 20%.

[22] J. L. Albacete, N. Armesto, J. G. Milhano, P. Q. Arias, and C. A. Salgado, Eur. Phys. J. C **71,** 1705 (2011).

[23] R. Arnaldi et al., Phys. Lett. B **706,** 263 (2012).

[24] I. Abt et al. (HERA-B Collaboration), Eur. Phys. J. C **60,** 525 (2009).

[25] E. G. Ferreiro, F. Fleuret, J.-P. Lansberg, N. Matagne, A. Rakotozafindrabe, arXiv:1110.5047.

[26] P. Amaudruz et al., Nucl. Phys. **B371,** 553 (1992).